



Broadband potential optimisation of a full scale acoustic metawindow performance

Gioia Fusaro¹
Department of Industrial Engineering, University of Bologna,
Viale Risorgimento 2, Bologna, 40136, Italy

Massimo Garai²
Department of Industrial Engineering, University of Bologna,
Viale Risorgimento 2, Bologna, 40136, Italy

Jian Kang³
Institute for Environmental Design and Engineering (IEDE), The Bartlett, University College
London, UK
Central House, 14 Upper Woburn Pl, London WC1H 0NN, United Kingdom

ABSTRACT

Noise control and airflow in duct-like systems are among some of the most interesting applications to conjugate AMMs innovation and sustainability. Specifically applied to the built environment, they opened up a new field of research supporting indoor wellbeing, sanitised environments, and public activities. Previous research conducted by the authors has proved AMM based window to be a resourceful way to address both natural ventilation and reduce the incoming noise propagation; however, the effective spectral range did not cover lower frequencies (50-350 Hz). For this reason, in the presented paper, implementation in the AMM unit geometry was performed over a full-scale acoustic metawindow (AMW). The resonating volume has been enhanced (by 200% of the original one) and coupled with a set of lateral flanks. Numerical analysis through FEM proved that on a range of opening ratio from 3 to 33%, the TL related to the window is improved overall of the 70% on the frequency range from 50 to 350 Hz. Such results encourage the use of new AMMs ergonomic windows in place of standard ones to achieve both natural ventilation and noise attenuation from 50 to 5k Hz, being resourceful for domestic, sanitary, and public applications.

1. INTRODUCTION

Metamaterials for noise control and ventilation are typically duct-like structures with embedded resonating systems on the side (eg. metasurfaces and metacages) and have originated for mechanical applications (mechanical engines isolation) [1,2]. In the latest decades, acoustic metamaterials (AMMs) have been used to cope with building engineering and indoor comfort issues such as noise

¹ gioia.fusaro@unibo.it

² massimo.garai@unibo.it

³ j.kang@ucl.ac.uk

transmission and ventilation [3]. Active and passive systems have been designed to improve indoor comfort, leading, for example, to mechanical ventilation and active noise control systems [4] or screening related systems (like rolling shutter boxes) [5]. However, these systems faced some limitations in terms of passive energetic requirements, broadband frequency range of application, and ergonomic value [6,7]. With this aim, the latest research development managed to achieve ergonomic driven window design based on acoustic metamaterials [8,9], which showed potential over ventilation and noise reduction but highlighted limitations over the lower frequency range. For these reasons, it is necessary to investigate further an ideal design of AMM based windows to address noise control and natural ventilation on a wider frequency range.

In a previous study investigating the potential of a full-scale AMW, Finite Element Method (FEM) was used to perform a parametric analysis (72 parametric analyses in total) [9]. Results showed effectiveness concerning two design parameters, frame's thickness and height (T and H in Figure 1.a), where a tailored AMM structure can achieve noise attenuation and increase or reduce opening time mostly without depending on the outdoor acoustic stimuli. Moreover, the previous study highlighted that models with $T=7.5, 10, 15$ and $H=0.05 - 0.15$ m can achieve interesting Transmission Loss (TL) values with optimal air change rate in minutes (ACRM), making this design suitable for most indoor public functions.

This study aims to optimise the performance of a full-scale AMM based window design broadening the frequency range of application to include the 50-350 Hz range, where the previous model showed limitations.

The tunability of the AMM unit cells constituting the metacage window, related to a few geometric parameters, has been demonstrated through previous parametric studies [10]; however, this original configuration did not consider the volume of the frame embedded corners in the following unit and full-scale AMM window. So, in this study, the AMM unit is implemented through perforation on the lateral flanks (Figure 1.b), which allows a significant increase in the resonating volume coupled with the rest of the AMW system. FEM was used to assess the TL optimisation of two different perforated configurations.

2. METHOD

2.1. Geometrical settings and broadband optimisation through resonating volume enhancement

As achieved in a previous study for the AMW unit [8], acoustic optimisation is investigated for the full-scale AMW design. In Fusaro et al. [8], three perforation configurations were tested numerically for the AMW unit for acoustic performance improvements in the lower frequency range. The resonating volume extension through AMM unit cells panels perforation was investigated to reach a resonance that affects low-frequency bandwidth. As a comparison, three configurations (configurations A, B, and C) with different perforating percentages and dispositions were studied and compared to the TL performance of the original frame model. Only the frame's corners' inner sides were modified accordingly with a 14% or 7% perforation ratio (where the percentage is calculated with the ratio between the whole inner panels' area and the perforated area). The perforation holes' diameter is $d = 6 \times 10^{-3}$ m. This parameter also represents the distance between each perforation hole (see Figure 1.b).

Since in the previous study, B and C Configurations resulted the most effective perforation combinations within the AMM unit's panels, optimisation on the full-scale AMW design is investigated following these two approaches. Configuration B has 7% perforation on the panels belonging to 2/4 of the same AMM units, while configuration C has 7% of the overall panels' area's perforation applied to one panel of each AMM unit. For the sake of simplicity in showing the results and since the previous section demonstrated that $H=0.05 - 0.15$ m performs optimally in noise reduction and natural ventilation, only these models will be tested. Moreover, since the $H=0.15$ m is quite a bulky window frame model which cannot be easily found on the market, this will be further excluded from the investigation. In the B and C Configurations, the resonating volume goes from $7.7 \times 10^{-4} \text{ m}^3$ ($H=0.05$ m) to $30.8 \times 10^{-4} \text{ m}^3$ ($H=0.10$ m), and the perforated panels within the AMW unit

geometry are placed differently to investigate also in this full-scale case if the perforation position is a determinant parameter for the AMW TL . As in previous studies, the thickness of the interior boundaries composing the AMW geometry is considered negligible.

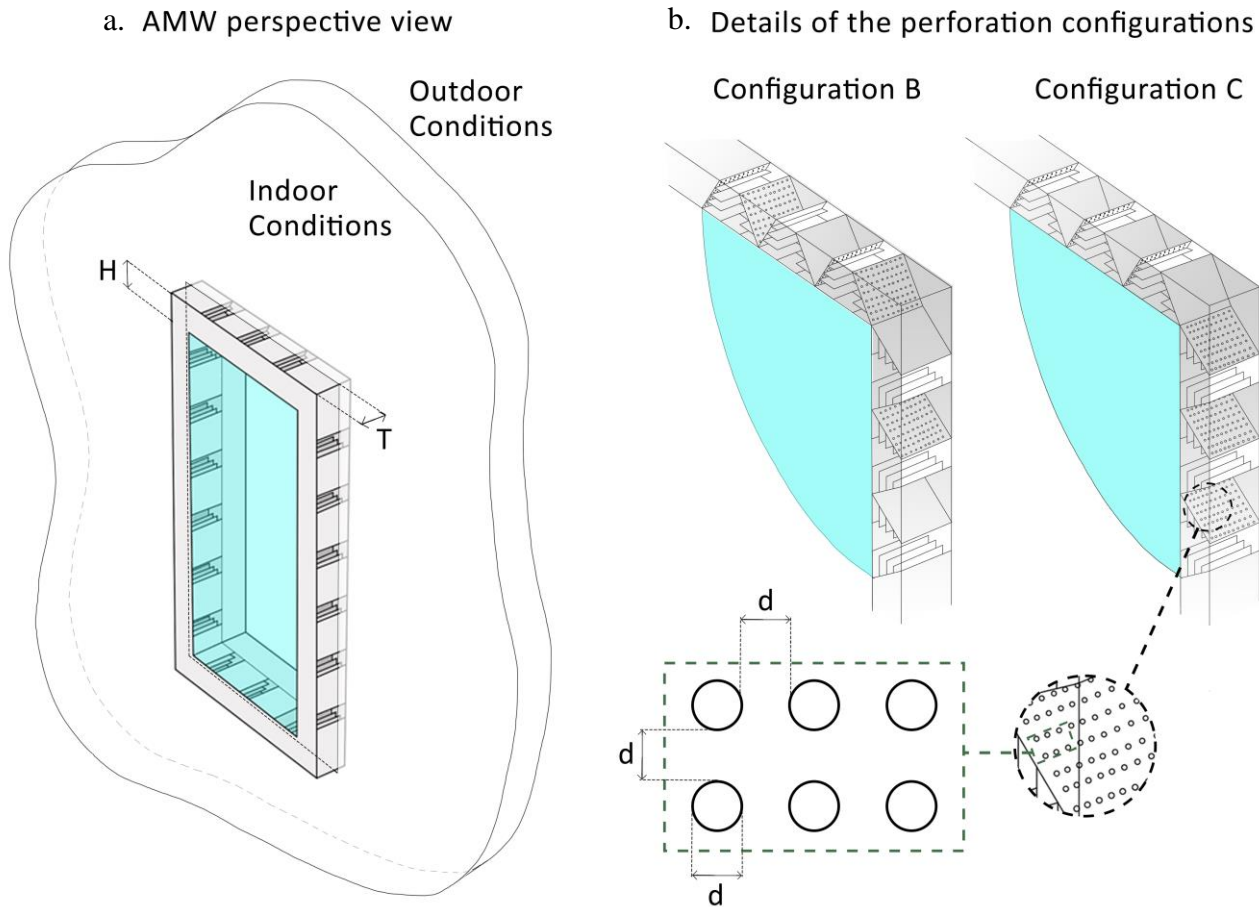


Figure 1 Schematics of a) full-scale AMW opening system and studied parameters (frame height, H , and thickness, T), and b) details of the perforation configurations B and C investigated in this study in order to optimise the low frequency range effectiveness. Hole diameter and distance $d=6 \times 10^{-3}$ m.

2.2 FEM model setup and boundary conditions

TL is here calculated through the numerical model, implemented using the commercial FEM software Comsol Multiphysics. The geometrical elements included are a spherical boundary of 0.9 m radius, a 0.13 m division in the middle (representing the building's wall), and the AMW attached to one side of the division. The sphere's partitions represent indoor and outdoor environments. Therefore, the AMW geometry is placed on the "inner wall". The dimension of the central transparent panel of the AMW is 1.2 x 0.6 m. The input wave (modelled as background pressure field) passes through the AMW and radiates in through the distributed ventilation holes along the AMM units' surface. As depicted in Figure 2.a, few parameters are considered for this study.

For the acoustic broadband investigation, semi-infinite acoustic conditions are applied to the two boundary sides of the sphere. Free spherical wave radiation conditions are applied to all the spherical geometry. The separation walls and the AMW geometry are characterised as interior sound hard boundaries. Sound transmission through walls of the AMW and possible viscous-thermal effect in the narrow resonator channels are neglected in this study. The 3D domain is filled with air, where air density and sound speed at room temperature are used. The outdoor boundary is characterised by a background pressure field directed towards the indoor with a pressure amplitude of 1 Pa and an airspeed of the sound of 343 m/s. TL is calculated by the reduction of sound power through the metamaterial interface (in dB). Regarding the mesh size for the 3D study, this model results very

complex, and since the convergence of results is proven, simplification is needed, so the maximum allowed element size is $343/6/2000=0.0286$ m. The study is a frequency domain analysis from 50 to 5000 Hz with a step size of 100 Hz. In the results, the TL is shown linearly within the simulation frequencies.

3. RESULTS

Figure 2 shows a comparison of the two schematics related to B and C Configurations TL characterised by $H=0.1$ m and $T=0.13$ m (a), $T=0.11$ m (b), $T=0.09$ m (c), $T=0.07$ m (d), $T=0.05$ m (e), $T=0.03$ m (f). These decreasing T values represent the closing mechanism of the AMW. So, from this schematics comparison, the effectiveness of TL can be appreciated simultaneously with the window opening reduction. Overall, B and C show significant TL throughout the whole frequency range (50-5000 Hz). The numerical analysis determines a minimum TL potential of 10 dB, which is particularly remarkable for the lower frequency range 50-500 Hz. Moreover, comparing the optimised configurations (B and C) with the RMS of the original full-scale AMW TL (represented by the red line plot), the TL optimisation is overall performed broadband in both cases. Specifically, configuration C shows better performance as it is clearly below the original AMW only in the frequency ranges of 1850-1900 Hz, while configuration B does not optimise TL at 1500-1600 Hz, 1850-1900 Hz, 3900-4100 Hz. Configuration C creates a resonant condition that optimises the system better than B. This is probably because perforated panels are not coupled. Indeed, an original AMM unit (cavities-based) configuration faces a perforated one (see Figure 2).

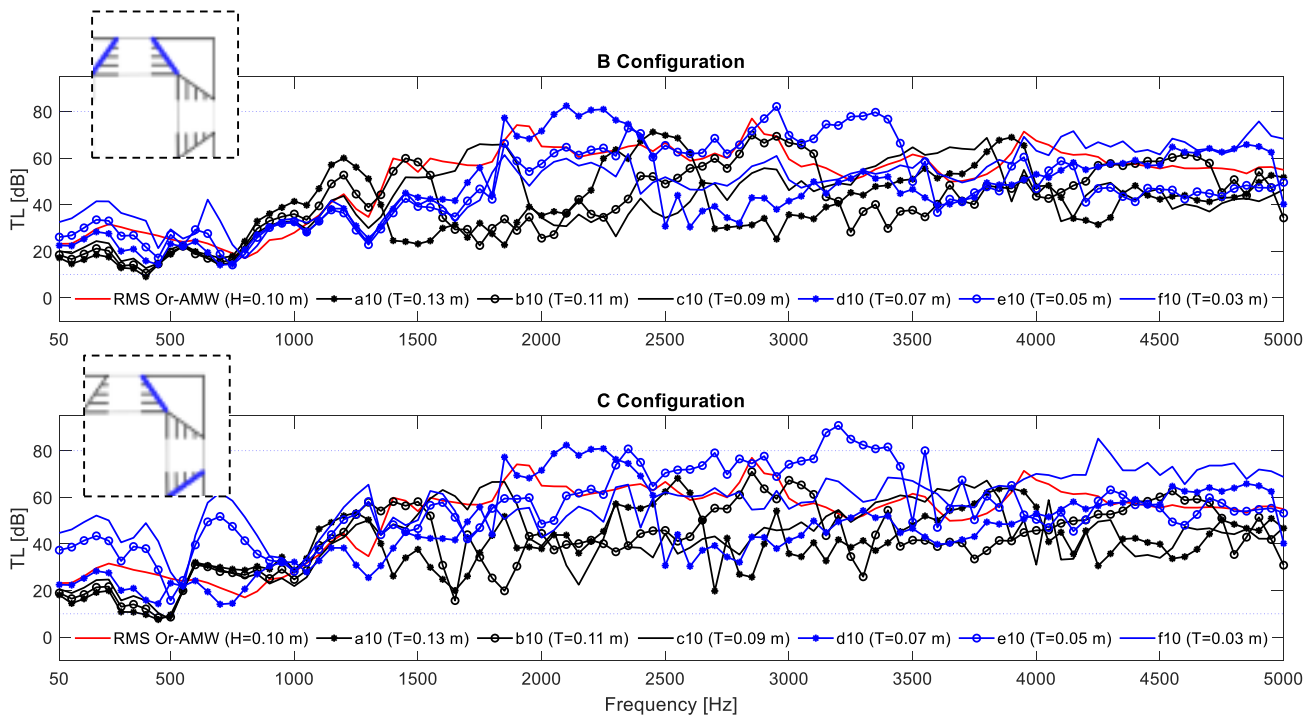


Figure 2 Schematics comparison of B and C Configurations TL characterised by $H=0.1$ m and $T=0.13$ m (a), $T=0.11$ m (b), $T=0.09$ m (c), $T=0.07$ m (d), $T=0.05$ m (e), $T=0.03$ m (f). Two blue dotted lines are plotted for $TL = 10$ dB and $TL= 80$ dB as reference for the overall TL performance. The red line plot represents the RMS of the original full-scale AMW TL. The solid blue line in the upper left corner detail represent the perforated flanks.

Figure 3 shows the optimised Configuration B and C TL of the full-scale AM, characterised by a frame height $H=0.075$ m. The decreasing value of T ($a=T=0.13$ m, $b=T=0.11$ m, $c=T=0.09$ m, $d=T=0.07$ m, $e=T=0.05$ m, $f=T=0.03$ m) represent the thickness of the window with constant H , and so the performance of the AMW at different degrees of closure. Overall, significant TL is highlighted from the numerical analysis of Configurations B and C. Also, in this case, C works better than B

generally throughout the frequency range 50-5000 Hz and specifically if compared with the TL RMS of the original AMW (represented by the red line plot). A significant dip is highlighted between 50 and 100 Hz for B, showing a magnification of the acoustic signal through this configuration for the bigger opening degrees ($T=0.13$, 0.11 , 0.09 m). It is possible to assume that, due to its even geometrical nature, Configuration C allows an optimised TL and overcomes possible magnifications as for B (see Figure 3).

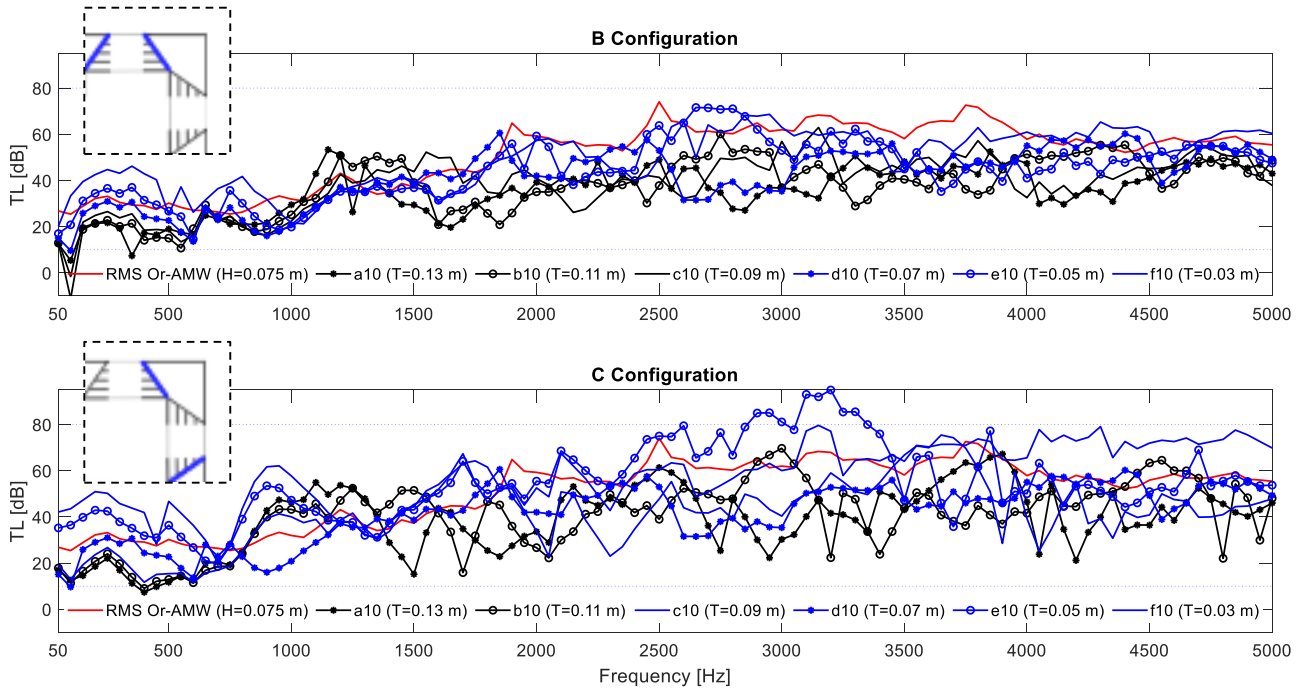


Figure 3 Schematics comparison of B and C Configurations TL characterised by $H=0.075$ m and $T=0.13$ m (a), $T=0.11$ m (b), $T=0.09$ m (c), $T=0.07$ m (d), $T=0.05$ m (e), $T=0.03$ m (f). Two blue dotted lines are plotted for $TL = 10$ dB and $TL= 80$ dB as reference for the overall TL performance. The red line plot represents the RMS of the original full-scale AMW TL. The solid blue line in the upper left corner detail represent the perforated flanks.

Figure 4 shows a comparison of the two schematics related to B and C Configurations TL characterised by $H=0.06$ m and decreasing T value represents the closing mechanism of the AMW ($a=T=0.13$ m, $b=T=0.11$ m, $c=T=0.09$ m, $d=T=0.07$ m, $e=T=0.05$ m, $f=T=0.03$ m). So, also for a frame thickness $H=0.06$ m, the effectiveness of TL can be appreciated simultaneously with the window opening reduction. Overall, B and C show significant TL throughout the 50-5000 Hz frequency range (minimum $TL=10$ dB and maximum $TL= 84$ dB). Clear advantages from Configuration C are shown from this numerical analysis, highlighting its merit again over B also in comparison with the RMS of the original full-scale AMW TL (represented by the red line plot). TL optimisation is indeed performed broadband by model C of the AMW (50-5000 Hz). Also, for a frame with $H=0.06$, Configuration C creates a resonant condition that optimises the system better than B because perforated panels are not coupled, and even AMM unit resonance is improved if compared with a mirrored one (see Figure 4).

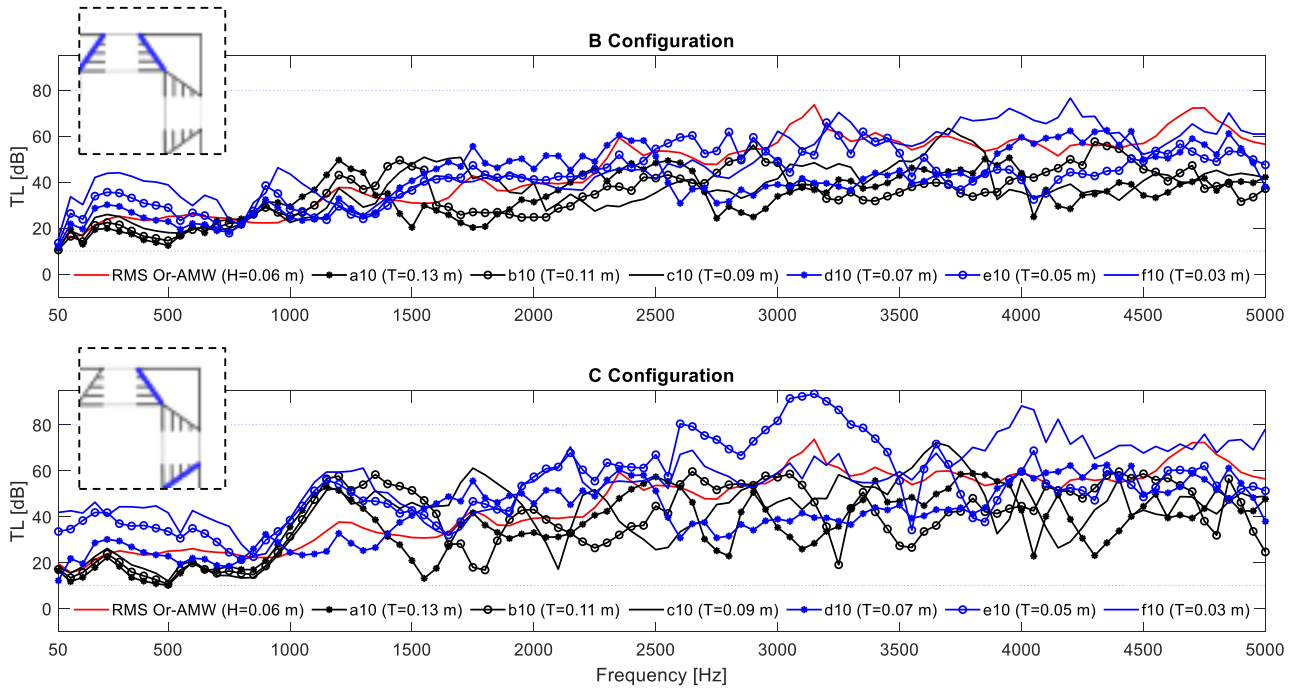


Figure 4 Schematics comparison of B and C Configurations TL characterised by $H=0.06$ m and $T=0.13$ m (a), $T=0.11$ m (b), $T=0.09$ m (c), $T=0.07$ m (d), $T=0.05$ m (e), $T=0.03$ m (f). Two blue dotted lines are plotted for $TL = 10$ dB and $TL= 80$ dB as reference for the overall TL performance. The red line plot represents the RMS of the original full-scale AMW TL. The solid blue line in the upper left corner detail represent the perforated flanks.

Finally, Figure 5 shows the TL of the optimised Configuration B and C of the full-scale AM, characterised by a frame height $H=0.05$ m. The decreasing value of T ($a=T=0.13$ m, $b=T=0.11$ m, $c=T=0.09$ m, $d=T=0.07$ m, $e=T=0.05$ m, $f=T=0.03$ m) represent the thickness of the window with constant H again, and so the performance of the AMW at different degrees of closure. Overall, significant TL is highlighted from the numerical analysis of Configurations B and C. Also, in this case, C works slightly better than B throughout the 50-5000 Hz frequency range, meaning that the smaller dimensions of the AMM unit within the frame neutralise the resonant contribution of the evenly perforated Configuration C. The comparison with the TL RMS of the original AMW (represented by the red line plot) shows overall merit toward the new optimised models (see Figure 5).

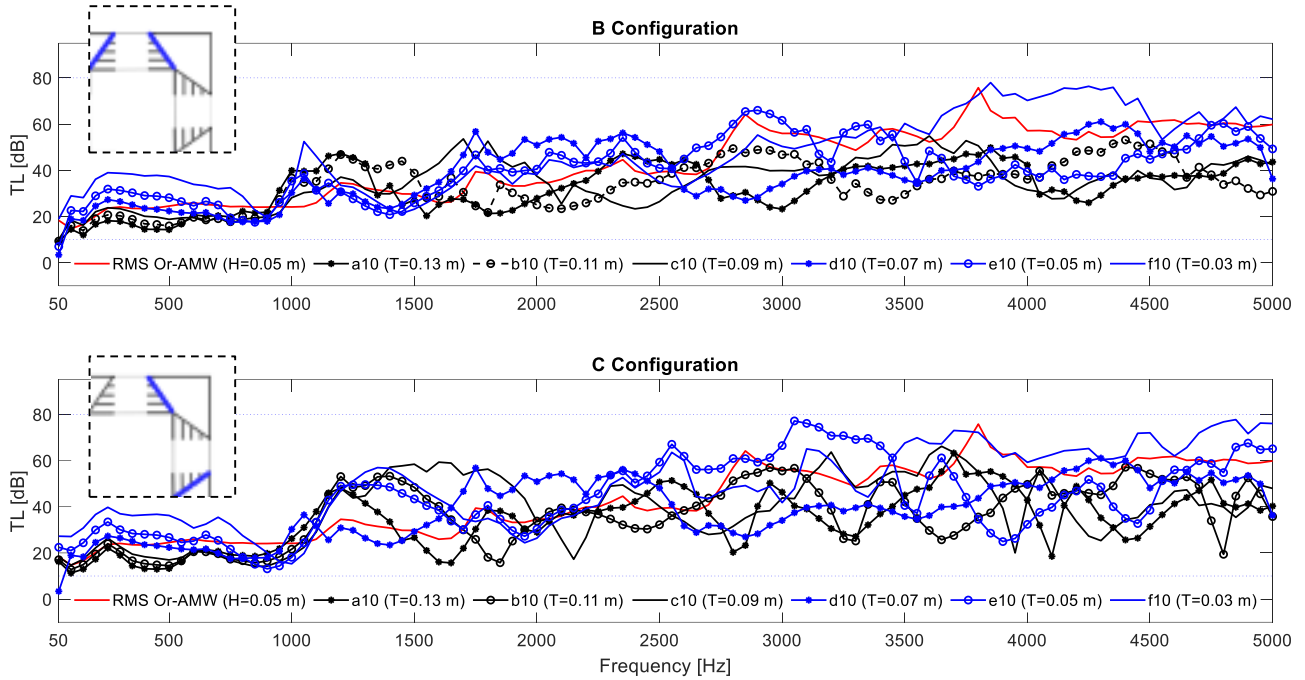


Figure 5 Schematics comparison of B and C Configurations TL characterised by $H=0.05$ m and $T=0.13$ m (a), $T=0.11$ m (b), $T=0.09$ m (c), $T=0.07$ m (d), $T=0.05$ m (e), $T=0.03$ m (f). Two blue dotted lines are plotted for $TL = 10$ dB and $TL= 80$ dB as reference for the overall TL performance. The red line plot represents the RMS of the original full-scale AMW TL. The solid blue line in the upper left corner detail represent the perforated flanks.

Overall, B and C Configurations work more efficiently when compared to the original configuration. In the case study of the full-scale AMW indeed, they allow the AMM unit to have the biggest resonating volume, showing that the perforation percentage is a crucial factor for the design of such an AMM window. This result is especially highlighted at low frequencies (50-500 Hz), where they reach an average of 25 dB of TL. On the other side, it is important to note that the perforated panels' disposition becomes more crucial with the increase of the frame height (H). It is possible to assume that, due to its even geometrical nature, Configuration C allows an optimised TL and overcomes limitations and even possible magnifications caused by B at a lower frequency range (50-100 Hz). Apart its acoustic merits over the original full-scale AMW model and the B variation, Configuration C might result in more convenient for an industrialised process since this specific design could allow a fabrication in series of the AMM unit pieces, which would be all the same. This feature would represent a great simplification in the fabrication process and so an advantage over production costs and time.

4. CONCLUSIONS

This study has attempted to explore the applicability of a previously developed AMW full-scale system for noise reduction and natural ventilation. A total of 48 parametric analyses have been carried out in order to assess the effectiveness concerning two design parameters: frame's thickness and height (T and H) for a broadband optimised AMW full-scale model.

First of all, from the acoustics point of view, the basic full-scale AMW reduces the incoming noise effectively with a minimum ΔTL of 1.5 dB and a maximum of 55.7 dB over a standard sliding window. Nevertheless, the noise reduction is guaranteed by the customisation of the AMW design (depending on H) and the degree of opening (depending on T).

The numerical analysis of the acoustically optimised model of AMW (in several different customisable designs according to T and H) finally shows that with a tailored perforated AMM unit structure [8], noise attenuation can be consistently achieved within the frequency range of 50-5000

Hz, and opening time can be increased or reduced mostly without depending on the outdoor acoustic stimuli. Furthermore, models with $T= 7.5, 10, 15$ m can achieve significant TL values with optimal air change rate in minutes (ACRM) (proved in the previous study), making this design suitable for most indoor public functions.

6. REFERENCES

1. Shen, C.; Xie, Y.; Li, J.; Cummer, S.A.; Jing, Y. Acoustic metacages for sound shielding with steady air flow. *J. Appl. Phys.* **2018**, *123*, 124501, doi:10.1063/1.5009441.
2. Jiménez, N.; Romero-García, V.; Pagneux, V.; Groby, J.P. Rainbow-trapping absorbers: Broadband, perfect and asymmetric sound absorption by subwavelength panels for transmission problems. *Sci. Rep.* **2017**, *7*, 1–12, doi:10.1038/s41598-017-13706-4.
3. Public Health England *Review and Update of Occupancy Factors for UK homes*; London, 2018;
4. Lam, B.; Shi, C.; Shi, D.; Gan, W.S. Active control of sound through full-sized open windows. *Build. Environ.* **2018**, *141*, 16–27.
5. Asdrubali, F.; Buratti, C. Sound intensity investigation of the acoustics performances of high insulation ventilating windows integrated with rolling shutter boxes. *Appl. Acoust.* **2005**, *66*, 1088–1101, doi:10.1016/j.apacoust.2005.02.001.
6. Lim, H.S.; Kim, G. The renovation of window mechanism for natural ventilation in a high-rise residential building. *Int. J. Vent.* **2018**, *17*, 17–30, doi:10.1080/14733315.2017.1351733.
7. Sorgato, M.J.; Melo, A.P.; Lamberts, R. The effect of window opening ventilation control on residential building energy consumption. *Energy Build.* **2016**, *133*, 1–13, doi:10.1016/j.enbuild.2016.09.059.
8. Fusaro, G.; Yu, X.; Lu, Z.; Cui, F.; Kang, J. A Metawindow with optimised acoustic and ventilation performance. *Appl. Sci.* **2021**, *11*, 1–16, doi:10.3390/app11073168.
9. Fusaro, G.; Group, A.; Tower, A.; Kingdom, U.; Yu, X.; Cui, F.; Kang, J.; Bartlett, T.; House, C.; Kingdom, U. Full-scale metamaterial window for building application. In Proceedings of the Inter-Noise 2020; Seoul, 2020.
10. Fusaro, G.; Yu, X.; Kang, J.; Cui, F. Development of metacage for noise control and natural ventilation in a window system. *Appl. Acoust.* **2020**, *170*, 107510, doi:10.1016/j.apacoust.2020.107510.